Applied Catalysis B: Environmental 126 (2012) 9–21

Contents lists available at SciVerse ScienceDirect

Applied Catalysis B: Environmental

journal homepage: www.elsevier.com/locate/apcatb

Mn–Fe/ZSM5 as a low-temperature SCR catalyst to remove NOx from diesel engine exhaust

Young Jin Kim[a], Hyuk Jae Kwon[a,1], Iljeong Heo[a], In-Sik Nam[a,*], Byong K. Cho[a], Jin Woo Choung[b], Moon-Soon Cha[c], Gwon Koo Yeo[c]

[a] Department of Chemical Engineering/School of Environmental Science and Engineering, Pohang University of Science and Technology (POSTECH), Pohang, Republic of Korea
[b] Power Train R&D Center, Cooperative & Development Division, Hyundai-Kia Motors, Hwaseong, Republic of Korea
[c] Technology Center, Ordeg Corporation, Ansan, Republic of Korea

ARTICLE INFO

Article history:
Received 16 March 2012
Received in revised form 11 June 2012
Accepted 12 June 2012
Available online 21 June 2012

Keywords:
Selective catalytic reduction
Manganese
Hydrothermal aging
Sulfur poisoning
HC inhibition

ABSTRACT

A Mn–Fe/ZSM5 catalyst has been developed for removing NOx from diesel engine exhausts and its excellent low-temperature SCR activity and N_2 selectivity demonstrated in comparison with other representative SCR catalysts including CuZSM5 and a Cu-based commercial catalyst (COM). The well-dispersed MnO_2 and the high NH_3 adsorption capacity of the Mn–Fe/ZSM5 catalyst have been identified as the primary sources for its high deNOx activity for NH_3/SCR. Hydrothermal stability and durability of the Mn–Fe/ZSM5 catalyst have been examined and compared to those of the CuZSM5 and COM catalysts. The hydrothermal stability of the catalyst improved upon the increase of Mn content and/or the addition of Er, the latter of which helps to stabilize the dispersion of MnOx on the catalyst surface during hydrothermal aging. The deNOx activity of the Mn–Fe/ZSM5 and its Er-promoted counterpart was less affected by HC poisoning, C_3H_6 poisoning in particular, compared to the CuZSM5 and COM catalysts, mainly due to the excellent C_3H_6 oxidation activity of MnO_2. No poisoning of the Mn-based ZSM5 and CuZSM5 catalysts has been observed upon the addition of 2 wt.% of K^+ and Ca^{2+} to their surface, primarily due to the high NH_3 adsorption capacity of the ZSM5 support, whereas the COM catalyst has been severely deactivated by the deposition of K^+ and Ca^{2+}. The deNOx activity of the Mn-based ZSM5 catalyst, particularly the Er-promoted one, was less affected by SO_2 compared to the CuZSM5 and COM catalysts, although it was hardly regenerated at 500 °C. Formation of $MnSO_4$ on the catalytic surface appears to be the primary cause for the deactivation of the Mn-based ZSM5 catalysts in the presence of SO_2 in the feed gas stream.

1. Introduction

Nitrogen oxide emission has become a primary concern among the air pollutants emitted from a diesel engine due to the difficulty of its removal under highly oxidizing conditions of the diesel engine exhaust. Selective catalytic reduction of NOx by urea (urea/SCR) is one of the most efficient technologies for removing NOx from diesel engine exhaust to meet ever-tightening emission regulations, including EURO VI and SULEV [1,2]. A catalyst for the urea/SCR technology is required to be active, especially in the low temperature region, since the normal exhaust gas temperature from a diesel engine ranging from 150 to 250 °C for light duty to 200–350 °C for heavy duty diesel engines is significantly lower than that from a gasoline engine, and the exhaust temperature from an advanced diesel engine for high fuel efficiency is expected to become even lower [3,4]. In addition, the urea/SCR catalyst should preferably maintain its initial activity against the dynamic and ever-changing diesel exhaust temperature and feed gas composition including SO_2 and HC emitted from the diesel engine [5–7].

CuZSM5, V_2O_5–WO_3/TiO_2 and FeZSM5 catalysts are representative catalysts employed for urea/SCR technology [8–10]. Among them, until recently, CuZSM5 has been known as the best low-temperature SCR catalyst [8]. Moreover, CHA (chabazite)-based catalysts, including CuSSZ13, have attracted special attention from the auto industry as a promising commercial catalyst for the urea/SCR system due to their excellent low-temperature activity and thermal stability [11,12]. However, the demand for new catalysts with enhanced low-temperature activity is expected to remain strong since the diesel exhaust temperature may further

* Corresponding author at: Department of Chemical Engineering/School of Environmental Science and Engineering, Pohang University of Science and Technology, San 31 Hyoja-dong, Pohang 790-784, Republic of Korea. Tel.: +82 54 279 2264; fax: +82 54 279 8299.
E-mail address: isnam@postech.ac.kr (I.-S. Nam).
[1] Present address: Energy Lab., Samsung Advanced Institute of Technology, San 14-1, Nongseo-dong, Giheung-gu, Yongin, Gyeonggi-do, 446-712, Republic of Korea.

0926-3373/$ – see front matter © 2012 Elsevier B.V. All rights reserved.
http://dx.doi.org/10.1016/j.apcatb.2012.06.010

decrease when the advanced combustion technology including homogeneous charge compression ignition (HCCI) is employed for the diesel engine [4].

Mn-based catalysts may provide an alternative catalytic system to address this issue. They have been reported as a low-temperature SCR catalyst, especially for the removal of NOx from stationary sources [13–18]. Recently, the Ni-doped Mn/TiO_2 has been developed as a promising catalytic system for removing NO by NH_3/SCR [19,20]. However, most of those Mn-based catalysts reported may not be suitable for the urea/SCR system to remove NOx from the diesel engine exhaust, since the deNOx activity of the Mn-based catalysts has been reported to be limited in a range of the reaction temperature from 80 to 250 °C and the reactor space velocity from 8000 to 30,000 h^{-1} in the absence of H_2O in the feed, which is far from the realistic diesel exhaust conditions [13–16]. Indeed, the comprehensive study on the hydrothermal stability of the Mn-based catalysts for the diesel application focused on catalyst sintering during the DPF regeneration period has rarely been reported. The hydrothermal stability, SO_2 and HC tolerance as well as the alkali metal resistance of the catalyst are important chemical characteristics to be investigated in developing a urea/SCR catalyst for the diesel exhaust after treatment system [5–7].

The hydrothermal stability of the urea/SCR catalyst is a critical issue, since the temperature of diesel exhaust containing H_2O may occasionally rise much higher than 600 °C during the regeneration of a DPF (diesel particulate filter) [21], which may sinter the SCR catalyst. Note that, depending upon the engine size, the urea/SCR system is commonly installed into the diesel exhaust treatment system right before or after the DPF [5]. The agglomeration of the active metal [22], the phase transition of the metal and catalyst support [23] and the migration of the reaction sites [21] as well as the dealumination of zeolite support [24] are among the primary causes for the thermal deactivation of the representative SCR catalysts including V_2O_5–WO_3/TiO_2 and zeolite-based catalysts. However, the hydrothermal stability of the Mn-based catalysts has been rarely reported, probably due to their commercial application primarily to stationary sources operating within a lower temperature range than the mobile sources. Urea/SCR catalysts may also be deactivated by SO_2 present in the exhaust gas stream from the diesel engine [6]. The deactivation is generally caused by the pore filling and blocking attributed to the formation of deactivation precursors such as NH_4HSO_4 and/or metal sulfates [25,26]. However, the sulfur tolerance of the urea/SCR catalyst for its automotive application has become less critical in recent years, as the concentration of SO_2 in the diesel exhaust gas stream becomes minimal due to the improvement of fuel quality [27]. When ULSD (ultra low sulfur diesel) is used for fuel, the concentration of SO_2 in the exhaust stream from the diesel engine is estimated to be in the range of 0.5 to 1 ppm [27].

On the other hand, HC (hydrocarbon) poisoning may be a new deactivation issue for the urea/SCR catalysts [28]. A significant amount of unburned HC species in the diesel exhaust may be expected during the cold-start period of the engine. Furthermore, the unburned HC may also slip even during its normal operating conditions, due to the deactivation of DOC (diesel oxidation catalyst) installed in the diesel after treatment system along with the urea/SCR [29,30]. Then, the NO reduction over the SCR catalyst may be inhibited by coking [7], competitive adsorption between NH_3 and HC [28,31] and side reactions such as ammoxidation [28].

The effect of alkali and alkaline earth metals on the deNOx activity over the urea/SCR catalyst is another important issue, since the lubrication oils, urea solution and diesel fuels commonly contain alkali and alkaline earth metals including K^+ and Ca^{2+} [32]. Those impurities decrease the deNOx activity of the SCR catalyst due to their deposition onto the acidic reaction sites on the catalyst surface [33].

In this study, a new generation of Mn–Fe/ZSM5 catalyst has been developed as a urea/SCR catalyst for removing NOx from diesel engine exhausts [34]. To evaluate the feasibility of the Mn–Fe/ZSM5 catalyst as a new commercial catalytic system for the urea/SCR technology, the catalytic activity of the Mn–Fe/ZSM5 catalyst has been directly compared to that of the representative SCR catalysts including other Mn-based catalysts, CuZSM5 as well as a Cu-based commercial catalyst (COM). In addition, the hydrothermal stability and durability of the Mn–Fe/ZSM5 catalyst have been systematically investigated, including the tolerance of the catalyst toward HC, SO_2, alkali and alkaline earth metals present in the diesel engine exhaust system. Physicochemical properties of the catalysts were characterized by XPS, FE-HRTEM, TGA, TPD and TPSR to understand and elucidate the deNOx activity as well as deactivation behavior of the NH_3/SCR catalysts.

2. Experimental

2.1. Catalyst preparation

Mn-, Fe-, and Er-based catalysts were prepared by impregnating ZSM5 (HSZ-830 NHA, NH_4^+ form; Si/Al = 14), TiO_2 (Hombikat UV100, Sachtleben) and γ-Al_2O_3 (CATALOX Sba-200, Sasol) supports with appropriate amounts of aqueous solutions of $Mn(NO_3)_2$, $Fe(NO_3)_2$ and $Er(NO_3)_2$, respectively, using the incipient wetness method. The metal contents were 20 or 30 wt.% of Mn, 10 wt.% of Fe and/or 10 wt.% of Er. The prepared catalysts were dried at 110 °C for 12 h in an oven followed by calcination at 500 °C for 5 h in airflow [34].

The Mn(3.0)ZSM5 and Cu(3.1)ZSM5 catalysts were prepared by the wet-ion exchange method using $Mn(NO_3)_2$ and $Cu(CH_3COO)_2$ as the metal precursors, respectively [8]. The Cu/zeolite-based commercial catalyst was provided by a catalyst manufacturer and denoted as COM in the present study. The COM powder was carefully scrapped off from the channel walls of the commercial SCR monolith catalyst for the deNOx activity test and characterization.

To investigate the hydrothermal stability of the catalysts, the samples were aged in a quartz tube reactor at 650 °C for 24 h with wet air containing 10% H_2O flowing at a rate of 1000 cm^3/min. The alkali metal-doped catalysts containing K^+ or Ca^{2+} were prepared by the incipient wetness impregnation method with aqueous solutions of K_2CO_3 or $CaCO_3$ [32], respectively. They were dried at 110 °C for 12 h and then calcined at 500 °C for 5 h. Listed in Table 1 are the catalysts prepared and tested in the present study, along with their physicochemical characteristics and metal contents.

2.2. Catalyst characterization

Specific surface areas of the catalysts were measured by the BET method with a sorption analyzer (ASAP 2010, Micromeritics Co.). X-ray photoelectron spectra (XPS) were obtained by using an ESCA spectrometer (ESCALAB 220iXL, VG-Scientific). The field emission-high resolution transmission electron microscopy (FE-HRTEM: JEM 2100F, JEOL) operated at 200 kV was employed to optically examine the dispersion of MnO_2 on the catalyst surface. Samples for the TEM study were prepared by dispersing the catalysts in ethanol, dropping them onto a holey carbon film supported on a copper grid and finally drying in an oven (110 °C). A thermogravimetric analysis (TGA) was conducted by an EXSTRA6000 TG system (SII Nano Technology Inc.) to identify the deactivating agents formed on the catalytic surface. The catalyst samples were heated from room temperature (RT) to 900 °C at 10 °C/min with flowing air (100 cm^3/min).

For the C_3H_6-TPSR analysis, the catalyst sample was pre-treated at 500 °C for 1 h with Ar, and cooled to RT. The sample was then flushed with 2000 ppm C_3H_6 in Ar balance for 1 h. Finally, the

Table 1
Physicochemical property of the catalysts employed in the present study.

Catalyst	Mn (wt.%)	Fe (wt.%)	Er (wt.%)	Cu (wt.%)	BET surface area ($m^2\ g^{-1}$)	Mn/SM[a]
TiO_2					338	
Al_2O_3					207	
ZSM5					352	
Mn(20)–Fe(10)/TiO_2	20	10			116	0.145
Mn(20)–Fe(10)/Al_2O_3	20	10			140	0.088
Mn(3.0)ZSM5[b]	3.0				335	
Mn(20)/ZSM5	20				250	0.084
Mn(20)–Fe(10)/ZSM5	20	10			220	0.214
Mn(30)–Fe(10)/ZSM5	30	10			184	0.274
Mn(30)–Fe(10)–Er(10)/ZSM5	30	10	10		170	0.282
Cu(3.1)ZSM5[b]				3.1	332	
COM[c]				2.8	390	
Fe(10)/ZSM5		10			280	
Mn(20)–Fe(10)/ZSM5 (aged)	20	10			206	0.145
Mn(30)–Fe(10)/ZSM5 (aged)	30	10			168	0.200
Mn(30)–Fe(10)–Er(10)/ZSM5 (aged)	30	10	10		150	0.261
Cu(3.1)ZSM5[b] (aged)				3.1	320	
COM[c] (aged)				2.8	382	

[a] Ratio of XPS atomic concentration (Mn/support metal: ZSM5, Al + Si; TiO_2, Ti; Al_2O_3, Al).
[b] Mn(3.0) and Cu(3.1)ZSM5 catalysts were prepared by ion-exchanged method.
[c] COM was provided by a catalyst manufacturer.

catalyst was heated to 800 °C at 10 °C/min in 5% O_2/Ar flow and the carbon-containing compounds including C_3H_6, CO and CO_2 were analyzed by an on-line mass spectrometer (QMI422/QME125, Pfeiffer/Balzers Quadstar). Before the NH_3-TPD analysis, the catalyst was pre-treated by the same procedure as the one used for the C_3H_6-TPSR study. In the NH_3-TPD experiments, NH_3 adsorption on the catalyst sample was carried out at RT using 1% NH_3/Ar flow followed by purging in Ar flow at the same temperature. The sample was then heated from RT to 800 °C at a ramping rate of 10 °C/min with flowing Ar, and the desorbed species were detected by a mass spectrometer.

2.3. Reaction system

The SCR activity was tested in a continuous fixed-bed flow reactor system (3/8-inch o.d. Al tube) with a feed gas typically containing 500 ppm NH_3, 500 ppm NO, 5% O_2, 10% H_2O and N_2 balance [8]. After the extensive study on the diffusion effect on the catalytic activity, 1 g of the catalyst powder in the 20/30 mesh size has been employed. NH_3 was used as the reductant for experimental convenience. Indeed, urea may readily decompose into NH_3 in the urea/SCR catalytic system [8]. Prior to each activity test, the catalysts were pretreated at 500 °C for 2 h with flowing air, and cooled to the initial reaction temperature around 150 °C. The steady-state deNOx activity test was then conducted in the reaction temperature range from 150 to 500 °C.

Note that the deNOx activity test in the present study was conducted at a high reactor space velocity of 100,000 h^{-1} over a wide reaction temperature window (150–500 °C), in order to simulate the realistic diesel exhaust condition.

The effect of HC poisoning on the deNOx activity was investigated by adding 500 ppm or 2000 ppm of C_3H_6 to the feed gas stream. The sulfur tolerance of the catalysts was investigated using a feed gas containing 1 ppm of SO_2, where SO_2 was continuously injected into the mixing zone made of glass beads right above the catalyst bed to avoid the formation of any sulfur compounds before the NH_3/SCR reaction. After 10 h of exposure of catalyst to sulfur, the SO_2 feed was cut off and the deNOx activity was then observed for 2 h without SO_2 to protect the analytical instruments from SO_2 contamination. The sulfated catalyst was regenerated in an airflow at 500 °C for 2 h, and then the catalytic activity was re-examined at the identical reaction condition. The inlet and outlet concentrations of NH_3, NO, NO_2, N_2O were determined by an on-line FT-IR (Nicolet 5700, Thermo Electron Co.) equipped with a 2 m gas-cell.

3. Results and discussion

3.1. DeNOx performance of Mn–Fe/ZSM5

The deNOx performance and N_2 selectivity of the Mn-based, CuZSM5, COM and FeZSM5 catalysts are depicted in Fig. 1. Upon the addition of Fe onto the Mn/ZSM5 catalyst, the NO conversion performance of the catalyst is enhanced in the low temperature region (<250 °C), while deteriorating in the high temperature region (>350 °C). The Mn–Fe/ZSM5 catalyst reveals a superior deNOx activity compared to the CuZSM5 and COM catalysts in the low temperature region; at 160 °C for instance, it achieves 80% of NO conversion compared to 40% and 30% over the CuZSM5 and COM, respectively. This is remarkable because both CuZSM5 and COM have been widely recognized as the best low-temperature SCR catalysts reported so far [8,11,12]. However, the NO conversion over the Mn–Fe/ZSM5 catalysts decreases below that over CuZSM5 and COM above 350 °C, probably due to the high oxidation activity of MnO_x resulting in the NH_3 oxidation by oxygen [35]. Thus, the Mn–Fe/ZSM5 catalyst may not be appropriate to remove NOx emitted from the diesel engine during the DPF regeneration involving a sudden increase of the diesel exhaust temperature above 500 °C. The regeneration of 10 min duration is typically conducted every 1000 km of the catalyst mileage [36]. However, the exhaust gas temperature of the next generation diesel engine based upon an advanced combustion system may be below 350 °C except for the DPF regeneration period, and the Mn–Fe/ZSM5 catalyst can maintain its excellent SCR activity including the high N_2 selectivity for reducing NOx within that temperature range, as clearly shown in Fig. 1. It is noteworthy that the Fe(10)/ZSM5 catalyst containing an identical Fe content (10 wt.%) prepared by the impregnation method and the Mn(3.0)ZSM5 catalyst prepared by the ion-exchange method exhibit negligible deNOx activities in the low temperature range.

As shown in Fig. 2, both Mn–Fe/TiO_2 and Mn–Fe/Al_2O_3 catalysts exhibit much lower deNOx activities and N_2 selectivities compared to those of the Mn–Fe/ZSM5 catalyst, even though the percentage loadings of Mn and Fe on the catalysts are the same at 20% and 10%, respectively. This indicates that the deNOx activity of the Mn–Fe based catalysts strongly depends on the catalyst support employed.

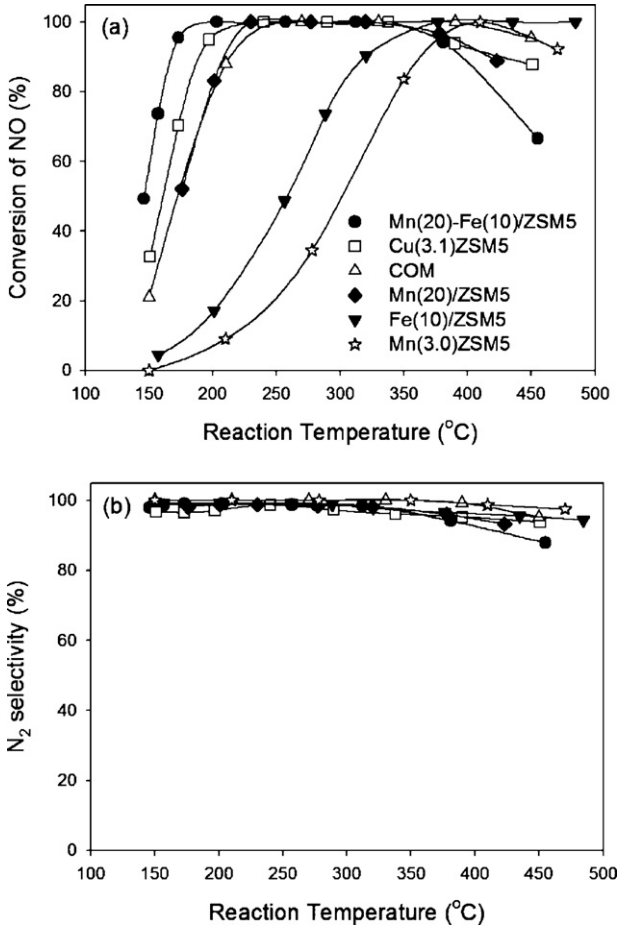

Fig. 1. DeNOx performance (a) and N_2 selectivity (b) over the Mn-based ZSM5, CuZSM5, COM and FeZSM5 catalysts. Feed condition: 500 ppm NH_3, 500 ppm NO, 5% O_2, 10% H_2O and N_2 balance; GHSV: 100,000 h^{-1}; N_2 selectivity of NO and NH_3 = [(conversion of NO + NH_3) − (formation of N_2O + NO_2)]/(conversion of NO + NH_3).

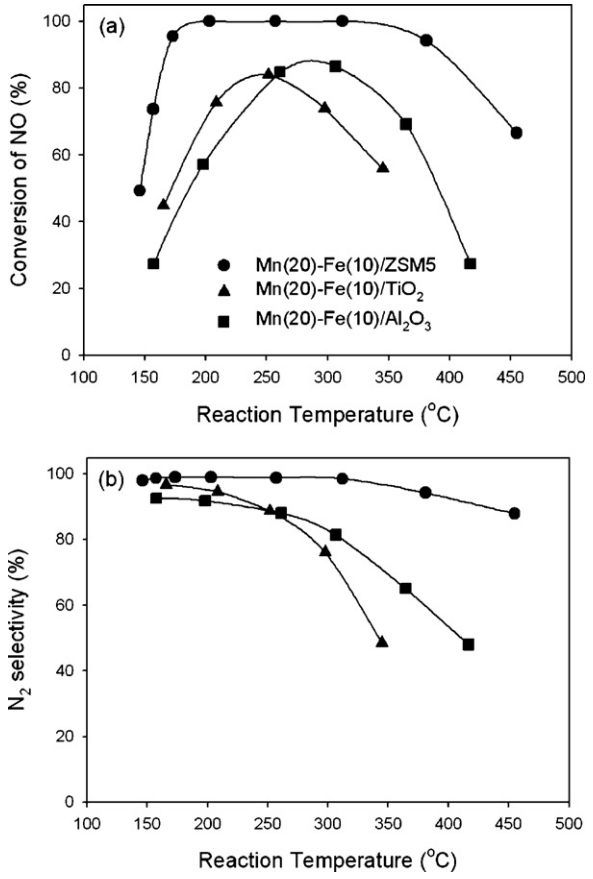

Fig. 2. Effect of support on Mn–Fe-based SCR catalysts: deNOx performance (a) and N_2 selectivity (b). Feed condition: 500 ppm NH_3, 500 ppm NO, 5% O_2, 10% H_2O and N_2 balance; GHSV: 100,000 h^{-1}; N_2 selectivity of NO and NH_3 = [(conversion of NO + NH_3) − (formation of N_2O + NO_2)]/(conversion of NO + NH_3).

The effect of the stored NH_3 on the deNOx activity may also be an important factor in developing an effective commercial urea/SCR catalyst [37], which has been investigated by transient response experiments (Fig. S1 in Supplementary Material). As NH_3 stored on the catalyst is consumed by its reaction with NO, the deNOx activity of the catalysts declines, and the decreasing rate of the Mn(20)–Fe(10)/ZSM5 catalyst activity is faster than that of the Cu(3.1)ZSM5 and COM catalysts. After NH_3 is added into the feed gas stream again, the Mn(20)–Fe(10)/ZSM5 catalyst recovers its deNOx performance in a shorter period of time, compared to the Cu(3.1)ZSM5 and COM catalysts. This result is closely related to the amount of NH_3 adsorbed and stored on the catalysts and the rate of SCR reaction consuming the stored NH_3.

Presented in Fig. 3 are XPS spectra collected to determine the state of Mn supported on ZSM5, TiO_2 and Al_2O_3. As shown in Figs. 3 and S2, Mn mainly exists as Mn^{4+} (641.9 eV) on the surface of the Mn-based catalysts, regardless of the catalyst supports employed

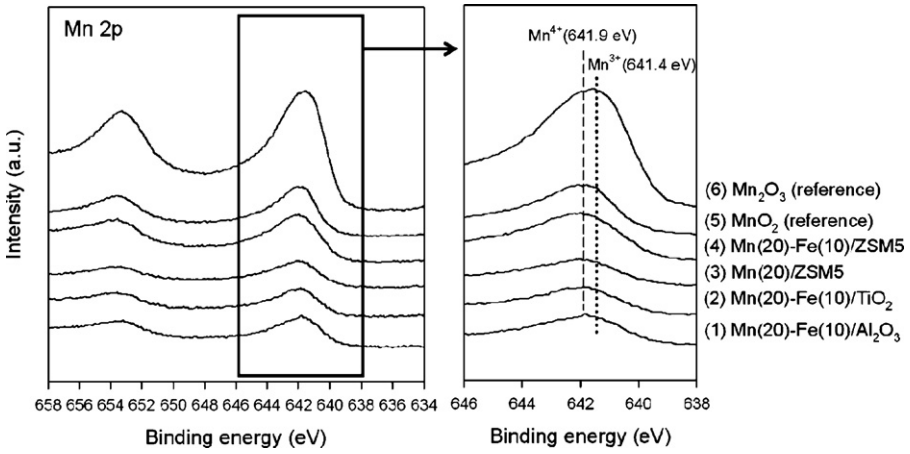

Fig. 3. XPS of Mn 2p core level. (1) Mn(20)–Fe(10)/Al_2O_3, (2) Mn(20)–Fe(10)/TiO_2, (3) Mn(20)/ZSM5, (4) Mn(20)–Fe(10)/ZSM5, (5) MnO_2 (reference) and (6) Mn_2O_3 (reference).

[38]. Fe loaded onto the catalysts exists in the form of Fe^{3+} as reflected in the Fe 2p spectra at 711.2 eV (Fig. S3). As also listed in Table 1, the atomic ratios of Mn/SM (manganese/support metal; Mn/(Al + Si), Mn/Ti or Mn/Al) on the surface of the catalysts were obtained from the XPS peak area of the elements contained in the catalysts. In general, the atomic Mn/SM ratio measured by XPS for a given total amount of MnO_2 increases with the enhanced dispersion of MnO_2 particles on the catalyst support [39], because the enhanced dispersion of MnO_2 results in an increased exposure of the MnO_2 surface accompanied by a decreased exposure of the support surface. The Mn/SM ratio of the Mn(20)/ZSM5 catalyst increases upon the addition of Fe, indicative of the increased dispersion of MnO_2 on the Mn–Fe based catalyst surface [39]. Moreover, the Mn(20)–Fe(10)/ZSM5 catalyst displays the highest Mn/SM ratio among the catalysts containing similar amounts of Mn and Fe, indicating that the dispersion of MnO_2 on the surface of the Mn–Fe/ZSM5 catalyst is superior to that of Mn–Fe/TiO_2, Mn–Fe/Al_2O_3 or Mn/ZSM5 catalysts. The Mn/SM ratio is well correlated with the low-temperature SCR activity in the temperature range below 250 °C. The increased dispersion of MnO_2 upon the addition of Fe has been confirmed by the TEM image as shown in Fig. 4. The dark colored particles represent MnO_2 and the bright ones are ZSM5 support. Large particles of MnO_2 are localized on the surface of Mn/ZSM5, whereas small ones are well dispersed on the surface of the Mn–Fe/ZSM5 catalyst. The improved dispersion of MnO_2 has been also determined by XRD patterns (Fig. S4). The peak of MnO_2 on the bimetallic Mn–Fe catalysts is much weaker and broader than that on the monometallic Mn catalysts, regardless of the catalyst support, which indicates that highly dispersed MnO_2 exists on the bimetallic Mn–Fe catalyst surface [15,40].

The nearly constant binding energy of the Mn 2p peak of the Mn(20)/ZSM5 and the Mn(20)–Fe(10)/ZSM5 observed in Fig. 3 suggests that Mn and Fe may reside on the Mn(20)–Fe(10)/ZSM5 as separate oxides, MnO_2 and Fe_2O_3 [41], without forming an Mn–Fe solid solution. The presence of Fe_2O_3 around MnO_2 on the Mn–Fe/ZSM5 catalyst surface may inhibit the agglomeration of MnO_2 during the catalyst sintering [15,42], resulting in the enhanced Mn dispersion.

The well-dispersed MnO_2 may readily oxidize NO to NO_2 or NO_3^- on the catalyst surface, and the "fast SCR" reaction ($4NH_3 + 2NO + 2NO_2 \rightarrow 4N_2 + 6H_2O$), which is much faster than the "standard SCR" reaction ($4NH_3 + 4NO + O_2 \rightarrow 4N_2 + 6H_2O$), may then proceed [2,9].

As shown in Fig. S5, the NO oxidation activity of the catalysts is well correlated with the dispersion of MnOx formed on the catalyst surface. Indeed, the oxidation of NO on the catalytic surface has been recognized as the rate-determining step of the SCR reaction over the zeolite-based catalyst [43], and the promoting effect of NO_2 on the deNOx activity can be clearly observed in Fig. S6. In addition, the inhibiting effect of NH_3 appears negligible on the Mn–Fe/ZSM5 catalyst, as depicted in Fig. S7 [44]. Thus, the well-dispersed MnO_2 on the surface of the Mn–Fe/ZSM5 catalysts is believed to be one of the primary reasons for its high deNOx performance at low temperatures.

The catalyst surface acidity also plays an important role for the urea/SCR (i.e., NH_3/SCR) reaction [45]. As shown in the NH_3-TPD results of Fig. 5, the Mn-based ZSM5 catalysts including Mn–Fe/ZSM5 and Mn/ZSM5 have a high NH_3 adsorption capacity, compared to the Mn–Fe/TiO_2 and Mn–Fe/Al_2O_3 catalysts, mainly due to the large number of surface acidic sites on the ZSM5 support. The large amount of the surface acidity of the Mn–Fe/ZSM5 catalyst appears to be another reason for its excellent deNOx activity. NH_3 is primarily adsorbed onto the Brønsted acid site formed on the surface of ZSM5, as clearly observed at 1449 and 1690 cm^{-1} of the IR wave number (Fig. S8) [46], with a small amount of NH_3 also adsorbed onto the Lewis acid sites on the surface of MnO_2 at 1591 cm^{-1} [38]. Although a similar amount of NH_3 is adsorbed on the Mn/ZSM5 and Mn–Fe/ZSM5 catalysts, the Mn–Fe/ZSM5 catalyst exhibits a better deNOx performance than the Mn/ZSM5 catalyst, probably due to the higher dispersion of Mn in the presence of Fe onto the bimetallic catalyst surface as discussed earlier. On the other hand, the amount of NH_3 adsorbed on Cu(3.1)ZSM5

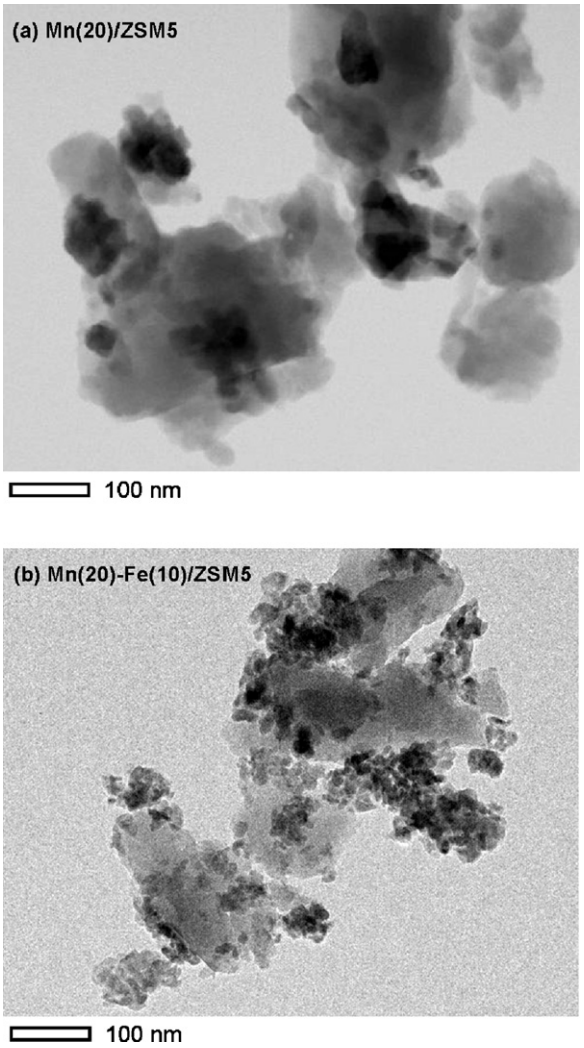

Fig. 4. TEM images of the Mn(20)/ZSM5 (a) and Mn(20)–Fe(10)/ZSM5 (b) catalysts.

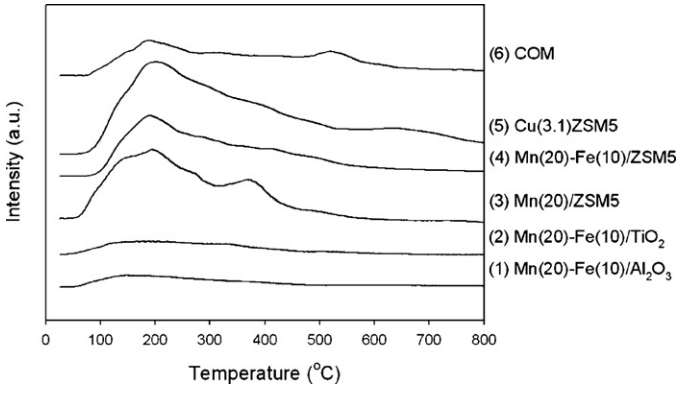

Fig. 5. NH_3-TPD over the catalysts. (1) Mn(20)–Fe(10)/Al_2O_3, (2) Mn(20)–Fe(10)/TiO_2, (3) Mn(20)/ZSM5, (4) Mn(20)–Fe(10)/ZSM5, (5) Cu(3.1)ZSM5, and (6) COM.

is larger than that on Mn(20)–Fe(10)/ZSM5, which is consistent with the slower rate of the change of the deNOx activity over the Cu(3.1)ZSM5 catalyst upon termination of NH_3 supply and re-start thereof, compared to that over the Mn(20)–Fe(10)/ZSM5 catalyst (Fig. S1). Although the COM catalyst has the smallest NH_3 adsorption capacity, the decreasing rate of its deNOx activity upon termination of NH_3 supply is slower than that of other catalysts. This can be attributed in part to its slower SCR reaction rate resulting in the relatively low deNOx activity at 200 °C, as clearly depicted in Fig. 1.

3.2. Hydrothermal stability

3.2.1. Effect of hydrothermal aging on deNOx performance

Presented in Fig. 6 is the NO removal activity of the Mn–Fe/ZSM5, CuZSM5 and COM catalysts before and after the hydrothermal aging at 650 °C for 24 h with flowing wet air containing 10% H_2O. The deNOx performance of the Mn(20)–Fe(10)/ZSM5 catalyst drastically decreases upon aging, from 100% to 20% at 200 °C in particular, presumably due to the transformation of MnO_2 to Mn_2O_3 occurring in the temperature range from 450 to 600 °C [47]. The agglomeration and sintering of MnO_x on the catalyst surface may be another cause for this thermal deactivation, which will be discussed in detail later. The dealumination of ZSM5 support can be ruled out as a cause for the thermal deactivation, based upon the ^{27}Al-MAS-NMR spectra of the Mn(20)/ZSM5 catalyst hydrothermally aged at 650 °C (Fig. S9a). Note that the resolution of the spectra of Mn–Fe/ZSM5 catalyst was too poor to distinguish the specific peaks, probably due to the interference of paramagnetic iron oxide included in the catalyst [48].

The deactivation of the Cu(3.1)ZSM5 is milder than that of the Mn(20)–Fe(10)/ZSM5; at 200 °C, the NO conversion decreased from 95% to 60% upon aging. The main cause for the sintering of the Cu(3.1)ZSM5 catalyst may be the migration of isolated Cu^{2+} [21]. Indeed, the dealumination hardly occurred over the aged CuZSM5 catalyst as well, as also shown in Fig. S9b, consistent with the results reported by Park et al. [21]. Interestingly, the COM catalyst is hardly deactivated by the hydrothermal treatment at 650 °C, and its catalytic activity may be further preserved even in harsher hydrothermal conditions [49].

However, the deactivation of the Mn–Fe/ZSM5 by the present hydrothermal aging is substantially mitigated by an increase of the catalyst Mn content from 20 wt.% to 30 wt.%. To further improve the hydrothermal stability of the Mn–Fe/ZSM5 catalyst, one of the rare earth metals such as Er has been impregnated onto the catalyst as a promoter [50]. Upon the addition of Er, the hydrothermal stability of the Mn–Fe/ZSM5 is further improved, as clearly observed in Fig. 6, confirming the beneficial role of Er in improving the hydrothermal stability of the Mn–Fe/ZSM5 catalyst [48]. Particularly, 80% of NO conversion is achieved at 200 °C over the aged Mn(30)–Fe(10)–Er(10)/ZSM5 catalyst, whereas only 20% over the aged Mn(20)–Fe(10)/ZSM5 catalyst.

3.2.2. Role of Mn and Er for improving the hydrothermal stability

To elucidate the improved hydrothermal stability of the Mn–Fe/ZSM5 catalyst upon the addition of Er, the XPS spectra of the Mn-based ZSM5 catalysts before and after hydrothermal aging were examined. As shown in Figs. 7 and S10, all the fresh Mn-based ZSM5 catalysts mainly reveal the peak assigned to Mn^{4+} (641.9 eV)

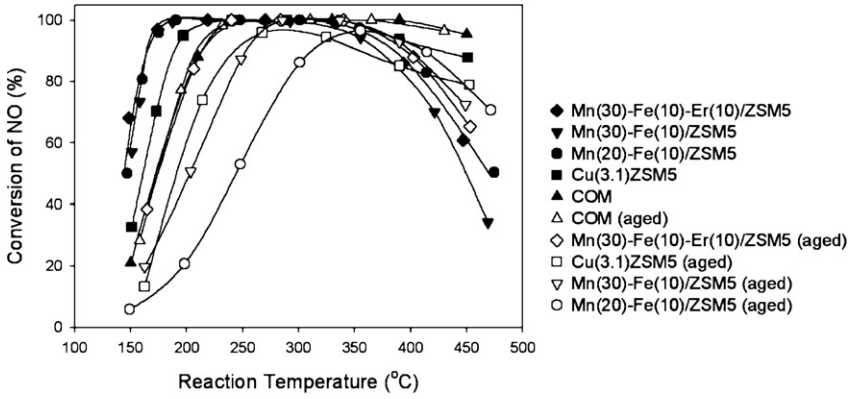

Fig. 6. Hydrothermal stability of the Mn-based ZSM5, CuZSM5 and COM catalysts. Feed condition: 500 ppm NH_3, 500 ppm NO, 5% O_2, 10% H_2O and N_2 balance. GHSV: 100,000 h^{-1}. Hydrothermal aging: at 650 °C for 24 h with flowing air containing 10% H_2O (2 L/min).

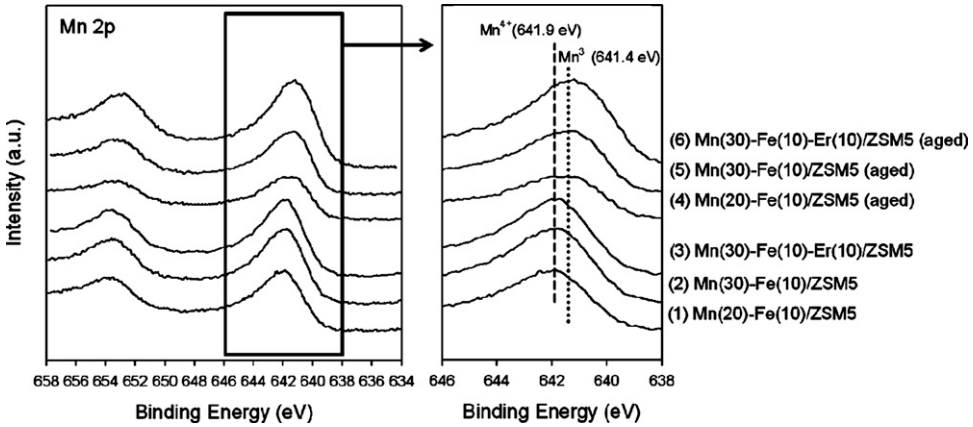

Fig. 7. XPS of Mn 2p core level. (1) Mn(20)–Fe(10)/ZSM5, (2) Mn(30)–Fe(10)/ZSM5, (3) Mn(30)–Fe(10)–Er(10)/ZSM5, (4) Mn(20)–Fe(10)/ZSM5 (aged), (5) Mn(30)–Fe(10)/ZSM5 (aged), and (6) Mn(30)–Fe(10)–Er(10)/ZSM5 (aged).

[38], reflecting that MnO_2 exists on the surface of the fresh catalysts as the primary phase of Mn. After aging, however, the main peak at 641.9 eV shifts to 641.4 eV corresponding to Mn^{3+} [51], indicating that MnO_2 is reduced to Mn_2O_3 during the hydrothermal aging. The alteration of Mn state has been also determined by XRD patterns (Fig. S11). The peak of MnO_2 on the catalysts has disappeared and new peaks assigned to Mn_2O_3 appeared after the hydrothermal aging. Thus, the phase transition of MnO_2 to Mn_2O_3 may be one of the causes for the hydrothermal deactivation of the Mn-based ZSM5 catalysts. Indeed, the deNOx activity of NH_3/SCR over MnO_2 has been shown to be generally superior to that over Mn_2O_3 [52].

Effect of aging on the Mn/SM ratios on the surface of the Mn-based ZSM5 catalysts can be found in Table 1. After aging, the Mn/SM ratio of the Mn(20)–Fe(10)/ZSM5 catalyst decreases from 0.214 to 0.146, indicating that the dispersion of MnOx on the surface of the catalyst decreases upon aging, and it may be another cause for the hydrothermal deactivation of the catalyst. The Mn/SM ratios of the Mn(30)–Fe(10)/ZSM5 catalyst before and after aging, 0.274 and 0.200, respectively, are higher than those of the Mn(20)–Fe(10)/ZSM5, resulting from the increased Mn content. Despite more Mn ions present on the surface of the Mn(30)–Fe(10)/ZSM5 catalyst compared to those on the Mn(20)–Fe(10)/ZSM5, the fresh SCR activity of the Mn(30)–Fe(10)/ZSM5 catalyst is similar to that over the Mn(20)–Fe(10)/ZSM5, especially in the low temperature region. Thus the amount of active Mn species on the surface of the Mn(20)–Fe(10)/ZSM5 may be enough for achieving the high deNOx activity, mainly due to the highly active MnO_2 on the fresh catalyst [53]. However, once MnO_2 is partly transformed to less active Mn_2O_3 upon aging, the amount of active Mn species on the surface of the Mn(20)–Fe(10)/ZSM5 may not be sufficient anymore to achieve a high deNOx activity. This may explain the low-temperature SCR activity over the aged Mn(30)–Fe(10)/ZSM5 catalyst that is higher than that over the aged Mn(20)–Fe(10)/ZSM5.

When Er is additionally impregnated onto the Mn(30)–Fe(10)/ZSM5 catalysts, the Mn/SM ratio of the catalyst decreases only slightly from 0.282 to 0.262 upon aging, indicating that Er helps to stabilize the MnOx dispersion during the hydrothermal aging. The effect of Er on the dispersion of MnOx can also be observed in the XRD patterns (Fig. S11). Much smaller and broader peaks attributed to Mn_2O_3 were observed over the Er-promoted catalyst after aging, indicating that the dispersion of MnOx has been enhanced [38,40]. Thus, the improved MnOx dispersion appears to be the primary reason for the enhanced hydrothermal stability of the Mn–Fe–Er/ZSM5 catalyst.

3.3. Poisoning by hydrocarbons in diesel engine exhaust

Presented in Fig. 8 is the effect of HC included in the diesel engine exhaust on the deNOx activity of the Mn-based ZSM5 catalysts. In the presence of 500 ppm C_3H_6 in the feed, the deNOx performance of the Mn-based ZSM5 catalysts – Mn(20)–Fe(10)/ZSM5 and

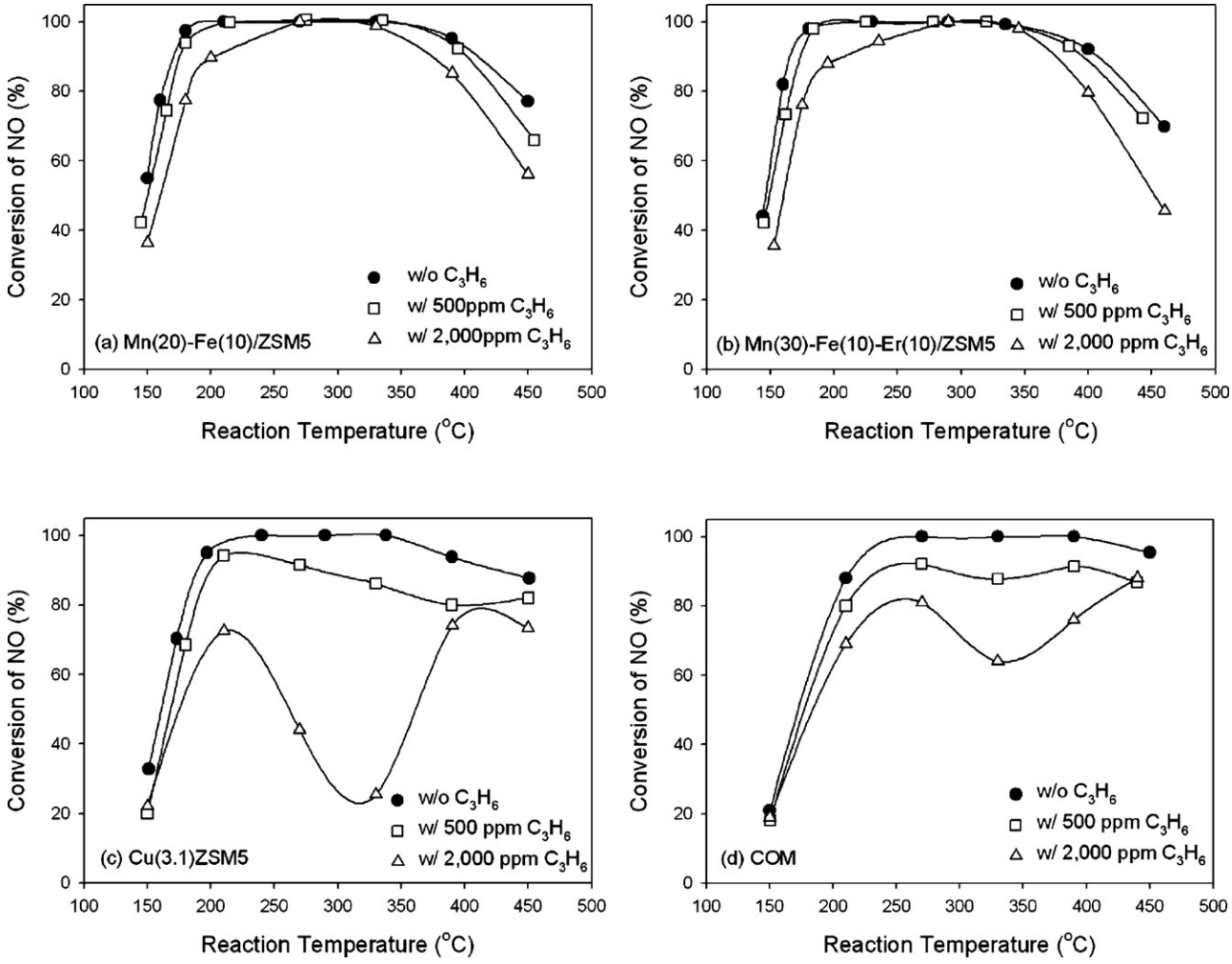

Fig. 8. Effect of C_3H_6 on the SCR reaction over the Mn(20)–Fe(10)/ZSM5 (a), Mn(30)–Fe(10)–Er(10)/ZSM5 (b), Cu(3.1)ZSM5 (c) and COM (d) by C_3H_6 inhibition. Feed condition: 500 ppm NH_3, 500 ppm NO, 5% O_2, 10% H_2O and 500 or 2000 ppm C_3H_6 and N_2 balance. GHSV: 100,000 h^{-1}.

Mn(30)–Fe(10)/ZSM5 – hardly decreases over the entire reaction temperature range (Fig. 8a and b), whereas noticeable decreases in the deNOx activity of the Cu-based catalysts – Cu(3.1)ZSM5 and COM – are observed (Fig. 8c and d). Poisoning of the Cu-based catalysts by C_3H_6 becomes more serious, particularly in the reaction temperature region from 200 °C to 400 °C, when the feed concentration of C_3H_6 increases from 500 ppm to 2000 ppm. Only 20% and 60% of NO conversion at 300 °C can be achieved over the Cu(3.1)ZSM5 and COM catalysts, respectively. In a sharp contrast, just a slight decrease of the deNOx activity is observed over the Mn-based ZSM5 catalysts, below 250 °C and above 350 °C. In particular, nearly 90% of NO conversion is obtained at 200 °C and 100% of NO conversion is still maintained at 300 °C, although 2000 ppm of C_3H_6 is added to the feed.

On the other hand, the decreased deNOx performance over the Cu-based catalysts increases again above 300 °C, presumably due to the HC/SCR reaction by C_3H_6 [28,54]. Indeed, both Cu-based catalysts show a reduction of NO by C_3H_6/SCR in the temperature range higher than 300 °C, whereas the Mn-based ZSM5 catalysts reveal HC/SCR activity between 200 and 400 °C (Fig. S12).

The primary cause for the deactivation of a urea/SCR system by C_3H_6 may be the strong adsorption of C_3H_6 onto the catalyst surface. Li et al. observed that the Fe^{3+} site on the surface of a FeZSM5 catalyst was blocked by C_3H_6, causing the NO oxidation activity over the catalyst to decrease, which resulted in the decline of the SCR activity [55]. Heo et al. recently reported that the decline of the deNOx performance over the SCR catalysts by the inclusion of C_3H_6 was attributable to not only the competitive adsorption of C_3H_6 and NH_3 but also a side reaction, ammoxidation between NH_3 and C_3H_6, leading to the unintended consumption of NH_3 [28]. Indeed, both Cu(3.1)ZSM5 and COM reveal higher conversions of NH_3 than those of NO, particularly in the temperature region of 250–400 °C, while both Mn(20)–Fe(10)/ZSM5 and Mn(30)–Fe(10)–Er(10)/ZSM5 exhibit a similar trend of excess NH_3 conversions above 350 °C, as also shown in Fig. S12. These excess NH_3 conversions beyond the NO conversion can be attributed to the combination of ammoxidation ($NH_3 + O_2 + C_3H_6$) and NH_3 oxidation ($NH_3 + O_2$) [28]. Note that the excess NH_3 conversion is not observed over the Mn-based ZSM5 catalysts in the medium temperature (250–350 °C), indicating that the ammoxidation reaction may hardly occur over these catalysts.

To further understand the cause for the stronger HC tolerance of the Mn-based ZSM5 catalysts, a C_3H_6-TPSR analysis was conducted. The desorption profiles of carbon-containing compounds including CO, CO_2 and C_3H_6 are shown in Fig. 9. The sharp peaks assigned to CO and CO_2 are observed at 210 °C over the Mn-based ZSM5 catalysts, while the broad peaks for the same compounds appeared at around 300 °C over the Cu(3.1)ZSM5 catalyst. It reflects the fact that the C_3H_6 adsorbed onto the Mn-based ZSM5 catalysts could be readily oxidized to CO and CO_2 at a temperature lower than that over the CuZSM5 catalyst, which is consistent with their C_3H_6 oxidation activity during the NH_3/SCR reaction in the presence of C_3H_6

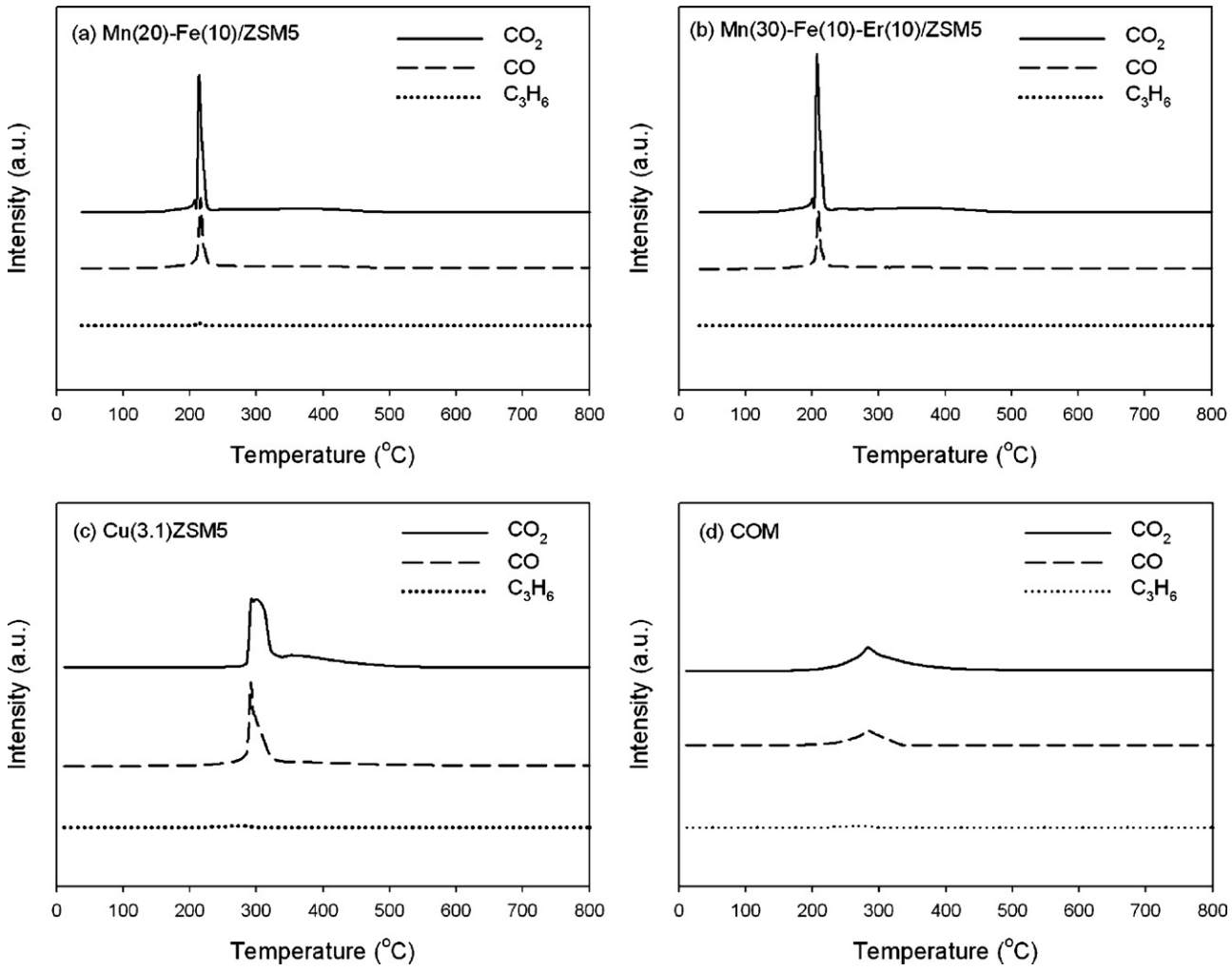

Fig. 9. The profiles of CO, CO_2 and C_3H_6 desorbed from the Mn(20)–Fe(10)/ZSM5 (a), Mn(30)–Fe(10)–Er(10)/ZSM5 (b), Cu(3.1)ZSM5 (c) and COM (d) catalysts during the course of C_3H_6-TPSR.

shown in Fig. S12. It is probably due to the superior oxidation activity of the MnO_2 formed on the surface of the Mn(20)–Fe(10)/ZSM5 [56], effectively removing from the catalyst surface the adsorbed C_3H_6, a deactivation precursor.

On the other hand, the peaks attributed to CO and CO_2 over the COM catalyst are observed at the similar temperatures to those over the CuZSM5 catalyst during the C_3H_6-TPSR analysis. However, their peak areas corresponding to the amount of the CO and CO_2 produced from the adsorbed C_3H_6 are much smaller than those over the CuZSM5 catalyst, indicating the COM catalyst adsorbed a smaller amount of C_3H_6 on its surface compared to the CuZSM5. This is consistent with the earlier observation that the NH_3/SCR reaction over the COM catalyst was less inhibited by C_3H_6 as shown in Fig. 8.

3.4. Poisoning of SCR catalysts by K^+ and Ca^{2+}

The effect of K^+ and Ca^{2+} commonly included in engine lubricants and urea solutions on the deNOx activity of the SCR catalysts was examined by impregnating 2 wt.% of K^+ and Ca^{2+} onto the catalysts, the result of which is shown in Fig. 10. The ZSM5-based Mn–Fe, Mn–Fe–Er and Cu catalysts exhibit a superior resistance to the poisoning by K^+ and Ca^{2+} (Fig. 10a–c) compared to the COM catalyst (Fig. 10d). The SCR activity of the ZSM5-based catalysts decreases only slightly upon the addition of K^+ onto the catalyst surfaces, while the inclusion of Ca^{2+} hardly affects the deNOx performance at all. However, the deNOx activity of the COM catalyst is reduced by 2 wt.% of Ca^+ doped onto its surface. The decline of its catalytic activity becomes more pronounced over the entire reaction temperature when 2 wt.% of K^+ is loaded onto the catalyst.

The decline of the deNOx performance over the SCR catalysts due to the deposition of K^+ and Ca^{2+} may be attributed to the alteration of the catalysts' surface acidity [33]. As mentioned, the catalyst surface acidity plays a critical role in the urea/SCR (NH_3/SCR) technology, since NH_3 is used as the reductant for removing NO [45]. To examine the alteration of the catalyst surface acidity upon the deposition of K^+ and Ca^{2+}, the NH_3-TPD analysis was conducted. As shown in Fig. 11, the ZSM5-based catalysts exhibit similar surface acidity. Upon the deposition of K^+ and Ca^{2+} onto the catalysts, the amount of the catalyst acidity measured by the peak area of NH_3 desorption decreases for all catalysts tested. However, the ZSM5-based catalysts still hold a significant amount and strength of the surface acidity. On the contrary, the surface acidity of the COM catalyst decreases substantially, when 2 wt.% of K^+ is deposited onto the catalyst surface, not to mention that the amount of catalyst surface acidity of the fresh COM is much less than that of the fresh ZSM5-based catalysts. This may be the primary reason behind the severe deactivation of the COM catalyst by the deposition of Ca^{2+} and K^+, and it can be concluded that the superior tolerance of the ZSM5-based catalysts toward the deposition of K^+ and Ca^{2+} is mainly due to the high NH_3 adsorption capacity of ZSM5 type zeolite employed as a catalyst support [57].

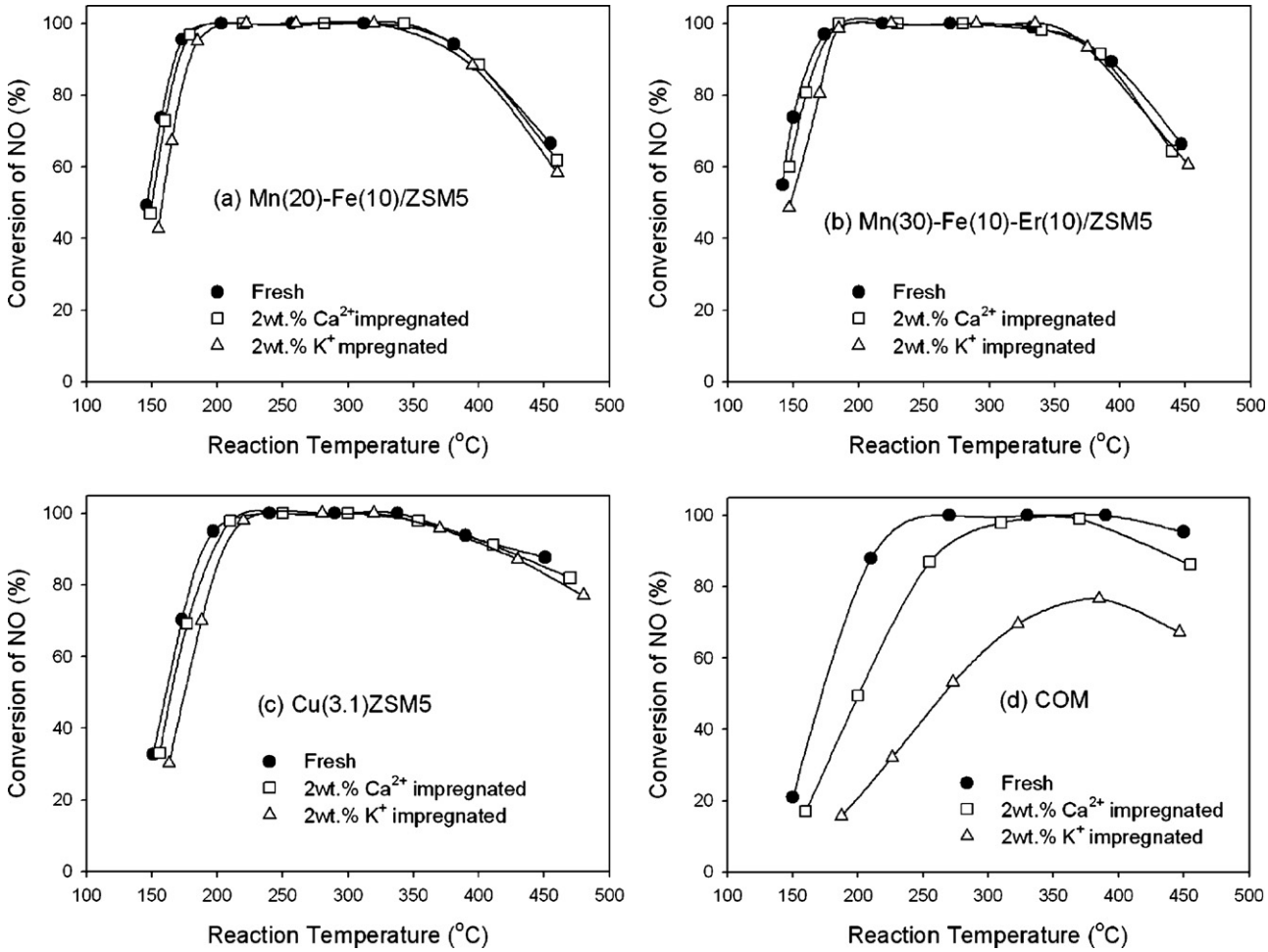

Fig. 10. The NO removal activity over the K^+- and Ca^{2+}-doped Mn(20)–Fe(10)/ZSM5 (a), Mn(30)–Fe(10)–Er(10)/ZSM5 (b), Cu(3.1)ZSM5 (c) and COM (d) catalysts. Feed condition: 500 ppm NH_3, 500 ppm NO, 5% O_2, 10% H_2O and N_2 balance. GHSV: 100,000 h^{-1}.

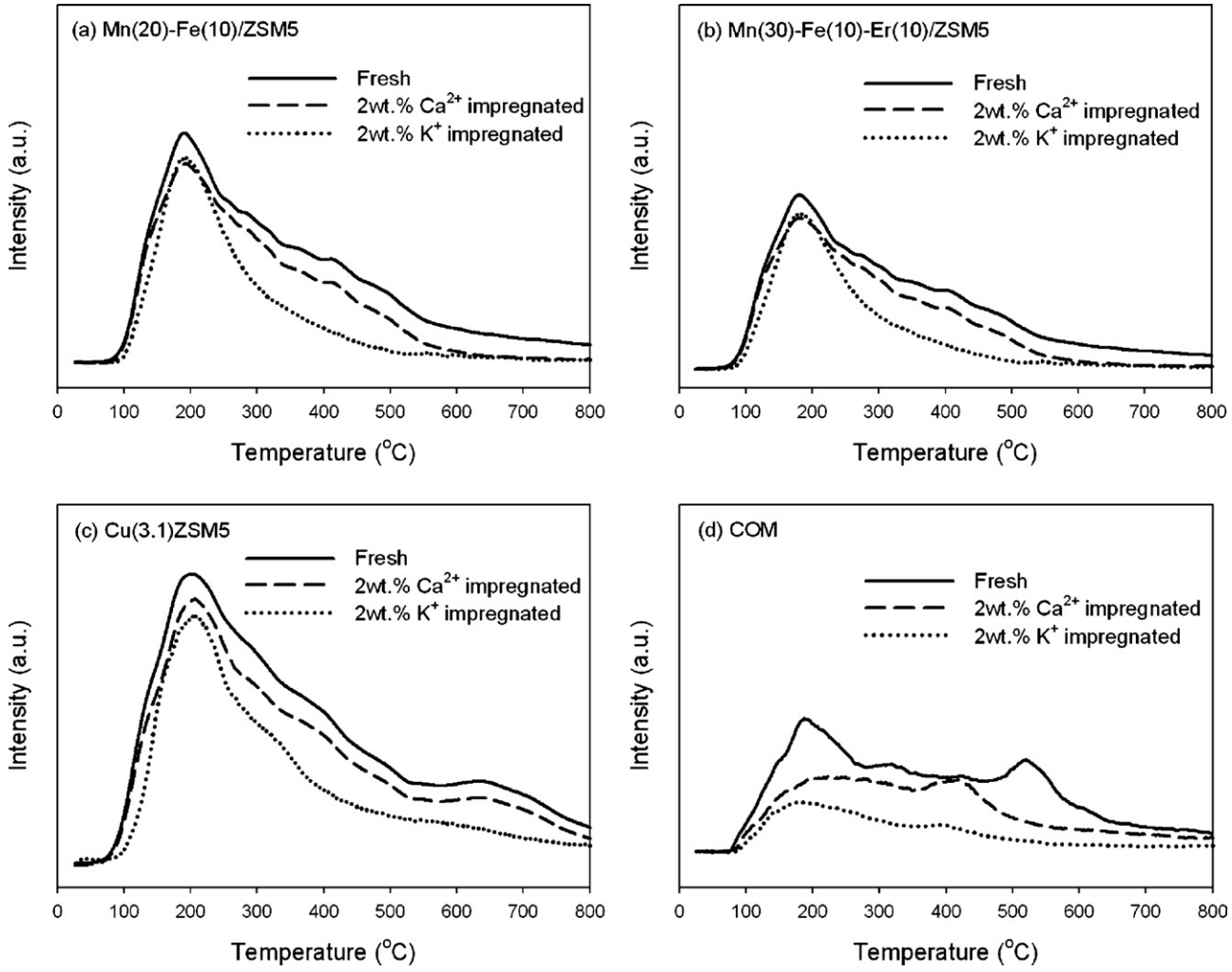

Fig. 11. NH_3-TPD over the K^+- and Ca^{2+}-doped Mn(20)–Fe(10)/ZSM5 (a), Mn(30)–Fe(10)–Er(10)/ZSM5 (b), Cu(3.1)ZSM5 (c) and COM (d) catalysts.

3.5. SO_2 tolerance of SCR catalysts

Sulfur tolerance has long been an important criterion in the development of an SCR catalyst for its application to the diesel after treatment system [25]. The effect of SO_2 on the deNOx activity of the Mn-based ZSM5, CuZSM5 and COM catalysts was examined at 200 °C and 270 °C using a feed stream containing 1 ppm SO_2 as illustrated in Fig. 12. The deNOx

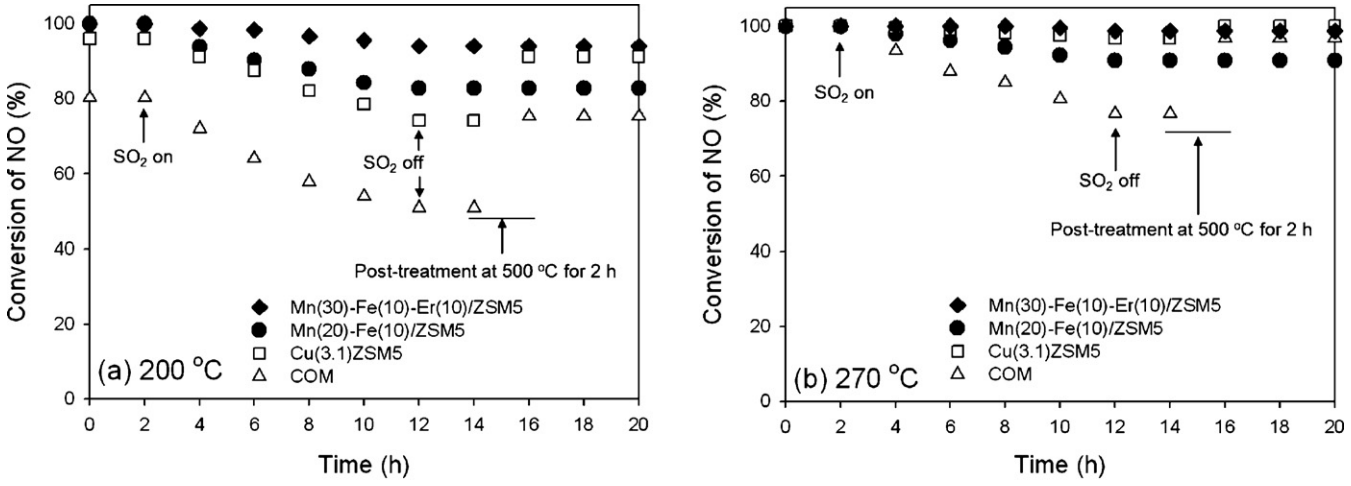

Fig. 12. Effect of SO_2 on the reduction of NO over the catalysts at 200 °C (a) and 270 °C (b). Feed condition: 500 ppm NH_3, 500 ppm NO, 5% O_2, 10% H_2O, 1 ppm SO_2 and N_2 balance. GHSV: 100,000 h^{-1}.

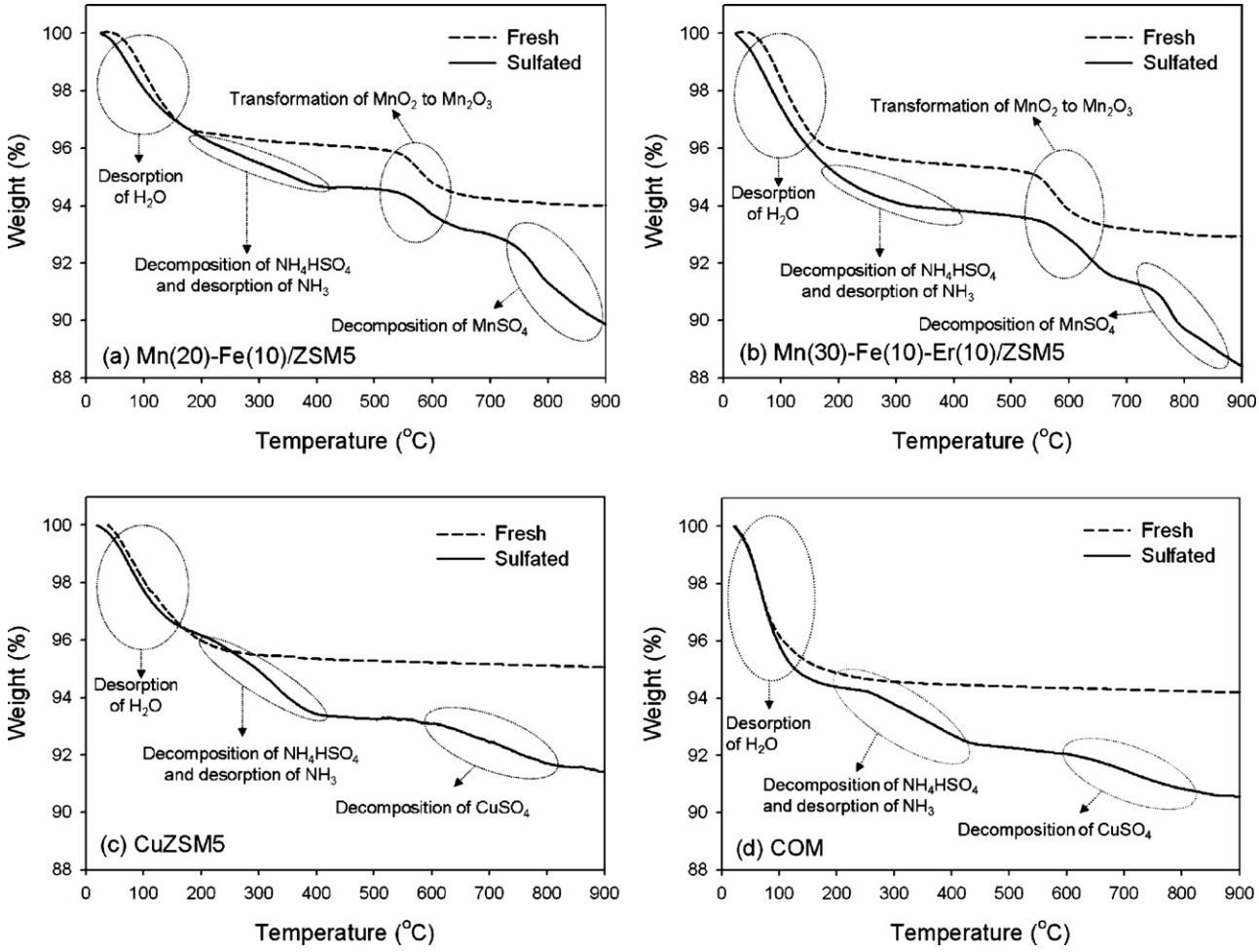

Fig. 13. TGA profiles of the Mn(20)–Fe(10)/ZSM5 (a), Mn(30)–Fe(10)–Er(10)/ZSM5 (b), Cu(3.1)ZSM5 (c) and COM (d) catalysts before/after the sulfation.

performance of all catalysts gradually decreases at both temperature, but more rapidly at 200 °C. The severity of the catalyst deactivation increases in the following order: Mn(30)–Fe(10)–Er(10)/ZSM5 < Mn(20)–Fe(10)/ZSM5 < Cu(3.1)ZSM5 < COM. Note that the NO conversion over the COM is reduced from 100% to 77% in 10 h, whereas more than 95% of NO conversion is still maintained over the Mn(30)–Fe(10)–Er(10)/ZSM5 catalyst at 270 °C. Thus, the catalytic activity of the Mn-based ZSM5 catalysts, particularly the Er-promoted counterpart, is less affected by SO_2 than that of the CuZSM5 and COM catalysts. However, the deNOx activity decreased by SO_2 is hardly restored over the Mn-based ZSM5 catalysts, while the deNOx performance of the Cu(3.1)ZSM5 and COM catalysts is nearly recovered, after the feed of SO_2 was cut off and the catalysts were treated with air at 500 °C for 2 h in air for regeneration. The long-term durability test over the Mn(30)–Fe(10)–Er(10)/ZSM5 catalyst has been also conducted in the presence of 1 ppm SO_2 at 200 °C as shown in Fig. S13. The deNOx activity over the catalyst decreases from 100% to 90% after 25 h, and 70% of NO conversion is obtained after 50 h of the reactor operation time in the presence of SO_2.

As mentioned, the deactivation of the SCR catalyst by SO_2 is generally caused by the formation of deactivation agents such as NH_4HSO_4 on the catalytic surface and/or the metal sulfate by the transformation of the active metal of the catalysts. The ammonium sulfates formed are known to decompose below 400 °C [58]. However, the sulfated Mn-based ZSM5 catalysts are hardly regenerated by the post-treatment at 500 °C, suggesting that the primary cause for the deactivation of the catalysts by SO_2 is not the formation of the ammonium sulfates but the formation of $MnSO_4$. Indeed, $MnSO_4$ was reported to decompose at the temperature higher than 750 °C [26]. On the other hand, the deactivating agents formed on the Cu(3.1)ZSM5 and COM are believed to be mostly the ammonium sulfates and $CuSO_4$ [6]. The activity of the Cu(3.1)ZSM5 and COM catalysts deactivated by SO_2 is nearly recovered, presumably by the decomposition of ammonium sulfates during the post-treatment at 500 °C.

To clarify the deactivating agent formed on the catalytic surface in the presence of SO_2, the TGA was performed. As shown in Fig. 13a and b, two temperature regions for the weight loss of the catalyst are observed over the Mn(20)–Fe(10)/ZSM5 and Mn(30)–Fe(10)–Er(10)/ZSM5 catalysts. The first one between RT and 150 °C corresponds to the desorption of H_2O from the catalyst surface. The other one from 550 °C to 650 °C is due to the transformation of MnO_2 to Mn_2O_3 on the catalytic surface releasing the structural oxygen in MnO_2 ($4MnO_2 \rightarrow 2Mn_2O_3 + O_2$) [47]. However, additional two weight loss regions are observed over the sulfated catalyst. The weight loss from 150 °C to 400 °C may be related to the decomposition of ammonium sulfate formed on the catalytic surface and/or the desorption of NH_3 [59], and another one from 750 °C is probably attributable to the decomposition of $MnSO_4$ [26,60], the latter of which indicates that MnO_2 has been transformed to $MnSO_4$ by SO_2 [26]. As mentioned, MnO_2 is known as the active reaction site for the low-temperature SCR. However, once MnO_2 is transformed to $MnSO_4$ by SO_2, NO_2 or NO_3 species can hardly be

adsorbed onto the catalytic surface and then the low-temperature SCR reaction does not occur effectively. That may be the primary reason for the deactivation of the Mn-based ZSM5 catalysts by SO_2.

On the other hand, the fresh CuZSM5 and COM catalysts reveal only one weight loss between RT and 150 °C, due to the desorption of H_2O. After the sulfation, two more regions of weight loss are observed; the first one from 150 °C to 400 °C is mainly due to the decomposition of ammonium sulfate and/or the desorption of NH_3, and the second one above 600 °C is probably due to the decomposition of $CuSO_4$ [61]. Although $CuSO_4$ is formed on the surface of Cu-based catalysts upon the inclusion of SO_2 in the feed, the primary deactivating precursor appears to be ammonium sulfates, since the Cu-based catalysts were readily regenerated by the post-treatment at 500 °C, as shown in Fig. 12.

The sulfur tolerance has been a critical issue for the Mn-based SCR catalysts [51,62]. Although the concentration of SO_2 in the diesel exhaust gas stream has been gradually lowered in recent years [27], a small amount of SO_2 may be still produced from diesel fuel as well as lubricating oil, and it can affect the deNOx activity of the Mn-based ZSM5 catalysts . The Mn-based ZSM5 catalysts developed in this study may require a regeneration procedure or need to be combined with a SOx trap for their successful implementation in the commercial urea/SCR system as a part of the after-treatment system for removing NOx from the diesel engine exhaust.

4. Conclusion

A Mn–Fe/ZSM5 exhibiting the high deNOx activity and N_2 selectivity over the operating temperature window of the diesel exhaust gas stream has been developed. The well-dispersed MnO_2 and the high surface acidity of the catalyst were found to be responsible for its high deNOx performance, as evidenced by XPS and NH_3-TPD analyses. To determine the feasibility of the Mn–Fe/ZSM5 catalyst in the application to the commercial diesel after treatment system, the hydrothermal stability and durability of the catalyst were also investigated. The deNOx activity of the Mn–Fe/ZSM5 catalyst for the NH_3/SCR decreased upon hydrothermal aging, due in part to the transformation of MnO_2 to Mn_2O_3 and in part to the sintering of MnOx on the catalyst surface. The hydrothermal stability of the Mn–Fe/ZSM5 catalyst was remarkably improved by the increase of Mn content and/or the addition of Er onto the catalyst. Er inhibited the agglomeration of the MnOx on the catalyst surface during the hydrothermal aging. The Mn-based ZSM5 catalysts such as Mn–Fe/ZSM5 and the Er-promoted counterpart exhibited superior resistance to deactivation induced by C_3H_6, compared to the CuZSM5 and COM catalysts. The excellent oxidation activity of the MnO_2 on the catalytic surface of the Mn-based ZSM5 catalysts appears to be the primary reason for the catalysts' high tolerance toward C_3H_6. The deNOx activity over the Mn-based ZSM5 catalysts or the CuZSM5 was hardly affected by the impregnated K^+ or Ca^{2+}, whereas that over the COM catalyst notably decreased upon the addition of K^+ or Ca^{2+} onto its surface. The NH_3-TPD result indicated that the strong tolerance of the ZSM5-based catalysts toward alkali or alkaline earth metal may be attributed to the high NH_3 adsorption capacity of the ZSM5 support.

In addition, the deNOx activity of the Mn-based ZSM5 catalysts, particularly the Mn–Fe–Er/ZSM5, was less affected by SO_2 compared to the CuZSM5 and COM catalysts. However, the deactivated Mn-based ZSM5 catalysts by SO_2 were hardly regenerated by the post-treatment at 500 °C for 2 h in air, suggesting the formation of $MnSO_4$ on the catalytic surface is the primary cause for the deactivation of the Mn-based ZSM5 catalysts by SO_2.

Acknowledgments

This work was supported by the Eco-Star Project under the supervision of the Ministry of Environment in Korea and the National Research Foundation of Korea (NRF) funded by the Ministry of Education, Science and Technology (MEST) (No. 2011-0029806).

Appendix A. Supplementary data

Supplementary data associated with this article can be found, in the online version, at http://dx.doi.org/10.1016/j.apcatb.2012.06.010.

References

[1] M.V. Twigg, Catalysis Today 163 (2011) 33.
[2] T.J. Wang, S.W. Baek, H.J. Kwon, Y.J. Kim, I.-S. Nam, M.-S. Cha, G.K. Yeo, Industrial and Engineering Chemistry Research 50 (2011) 2850.
[3] R.G. Gonzales, Diesel exhaust emission system temperature test, T&D report 0851-1816P, U.S. Department of Agriculture, 2008.
[4] D.S. Kim, C.S. Lee, Fuel 85 (2006) 695.
[5] T.J. Toops, K. Nguyen, A.L. Foster, B.G. Bunting, N.A. Ottinger, J.A. Pihl, E.W. Hagaman, J. Jiao, Catalysis Today 151 (2010) 257.
[6] Y. Cheng, C. Lambert, D.H. Kim, J.H. Kwak, S.J. Cho, C.H.F. Peden, Catalysis Today 151 (2010) 266.
[7] C. He, Y. Wang, Y. Cheng, C.K. Lambert, R.T. Yang, Applied Catalysis A-General 368 (2009) 121.
[8] J.H. Baik, S.D. Yim, I.-S. Nam, Y.S. Mok, J.-H. Lee, B.K. Cho, S.H. Oh, Topics in Catalysis 30 (2004) 37.
[9] P. Forzatti, I. Nova, E. Tronconi, Angewandte Chemie International Edition 48 (2009) 8366.
[10] S. Brandenberger, O. Kröcher, A. Tissler, R. Althoff, Applied Catalysis B: Environmental 95 (2010) 348.
[11] D.W. Fickel, E. D'Addio, J.A. Lauterbach, R.F. Lobo, Applied Catalysis B: Environmental 102 (2011) 441.
[12] J.H. Kwak, R.G. Tonkyn, D.H. Kim, J. Szanyi, C.H.F. Peden, Journal of Catalysis 275 (2010) 187.
[13] P.G. Smirniotis, D.A. Peña, B.S. Uphade, Angewandte Chemie International Edition 40 (2001) 2479.
[14] G. Qi, R.T. Yang, Journal of Physical Chemistry B 108 (2004) 15738.
[15] G. Qi, R.T. Yang, Applied Catalysis B: Environmental 44 (2003) 217.
[16] J. Huang, Z. Tong, Y. Huang, J. Zhang, Applied Catalysis B: Environmental 78 (2008) 309.
[17] Z. Chen, Q.Q. Yang, H. Li, X. Li, L. Wang, S.C. Tsang, Journal of Catalysis 276 (2010) 56.
[18] S. Yang, C. Wang, J. Li, N. Yan, L. Ma, H. Chang, Applied Catalysis B: Environmental 110 (2011) 71.
[19] B. Thirupathi, P.G. Smirniotis, Applied Catalysis B: Environmental 110 (2011) 195.
[20] B. Thirupathi, P.G. Smirniotis, Journal of Catalysis 288 (2012) 74.
[21] J.H. Park, H.J. Park, J.H. Baik, I.-S. Nam, C.H. Shin, J.-H. Lee, B.K. Cho, S.H. Oh, Journal of Catalysis 240 (2006) 47.
[22] M.A.L. Vargas, M. Casanova, Al. Trovarelli, G. Busca, Applied Catalysis B: Environmental 75 (2007) 303.
[23] J.W. Choung, I.-S. Nam, S.-W. Ham, Catalysis Today 111 (2006) 242.
[24] T. Tanabe, T. Iijima, A. Koiwai, J. Mizuno, K. Yokota, A. Isogai, Applied Catalysis B: Environmental 6 (1995) 145.
[25] B.-W. Soh, I.-S. Nam, Industrial and Engineering Chemistry Research 42 (2003) 2975.
[26] W.S. Kijlstra, M.B. Biervliet, E.K. Poels, A. Bliek, Applied Catalysis B: Environmental 16 (1998) 327.
[27] O. Kröcher, M. Widmer, M. Elsener, D. Rothe, Industrial and Engineering Chemistry Research 48 (2009) 9847.
[28] I. Heo, Y. Lee, I.-S. Nam, J.W. Choung, J.-H. Lee, H.-J. Kim, Microporous and Mesoporous Materials 141 (2011) 8.
[29] D. Ganesh, G. Nagarajan, M.M. Ibrahim, Fuel 87 (2008) 3497.
[30] J. Andersson, M. Antonsson, L. Eurenius, E. Olsson, M. Skoglundh, Applied Catalysis B: Environmental 72 (2007) 71.
[31] I. Malpartida, O. Marie, P. Bazin, M. Daturi, X. Jeandel, Applied Catalysis B: Environmental 102 (2011) 190.
[32] O. Kröcher, M. Elsener, Applied Catalysis B: Environmental 75 (2008) 215.
[33] S.S.R. Putluru, A. Riisager, R. Fehrmann, Applied Catalysis B: Environmental 101 (2011) 183.
[34] J.W. Choung, I.-S. Nam, H.J. Kwon, Y.J. Kim, D.-H. Kang, M.-S. Cha, US Pat., 8,048,393 B2 (November 01, 2011).
[35] K. Krishna, G.B.F. Seijger, C.M. van den Bleek, H.P.A. Calis, Chemical Communications (2002) 2030.
[36] H. Dwyer, A. Ayala, S. Zhang, J. Collins, T. Huai, J. Herner, W. Chau, Journal of Aerosol Science 41 (2010) 541.

[37] G. Guo, J. Warner, G. Cavataio, D. Dobson, E. Badillo, C. Lambert, SAE technical paper, 2010-01-1183 (2010).
[38] D.A. Peña, B.S. Uphade, P.G. Smirniotis, Journal of Catalysis 221 (2004) 421.
[39] J. Yu, F. Guo, Y. Wang, J. Zhu, Y. Liu, F. Su, S. Gao, G. Xu, Applied Catalysis B: Environmental 95 (2010) 160.
[40] Y.J. Kim, H.J. Kwon, I.-S. Nam, J.W. Choung, J.K. Kil, H.-J. Kim, M.-S. Cha, G.K. Yeo, Catalysis Today 151 (2010) 244.
[41] X. Tang, Y. Li, X. Huang, Y. Xu, H. Zhu, J. Wang, W. Shen, Applied Catalysis B: Environmental 62 (2006) 265.
[42] A. Morikawa, T. Suzuki, T. Kanazawa, K. Kikuta, A. Suda, H. Shinjo, Applied Catalysis B: Environmental 78 (2008) 210.
[43] L. Olsson, H. Sjövall, R.J. Blint, Applied Catalysis B: Environmental 87 (2009) 200.
[44] J.-Y. Luo, X. Hou, P. Wijayakoon, S.J. Schmieg, W. Li, W.S. Epling, Applied Catalysis B: Environmental 102 (2011) 110.
[45] E.Y. Choi, I.-S. Nam, Y.G. Kim, Journal of Catalysis 161 (1996) 597.
[46] R.Q. Long, R.T. Yang, Journal of the American Chemical Society 121 (1999) 5595.
[47] W.M. Shaheen, K.S. Hong, Thermochimica Acta 381 (2002) 153.
[48] P. Marturano, L. Drozdová, A. Kogelbauer, R. Prins, Journal of Catalysis 192 (2000) 236.
[49] G. Cavataio, H.-W. Jen, J.R. Warner, J.W. Girard, J.Y. Kim, C.K. Lambert, SAE technical paper, 2008-01-1025 (2008).
[50] J.W. Choung, J.K. Kil, I.-S. Nam, M.-S. Cha, H.J. Kwon, Y.J. Kim, D.-H. Kang, Kor. Pat., 1126247 (March 06, 2012).
[51] B.J. Tan, K.J. Klabunde, P.M.A. Sherwood, Journal of the American Chemical Society 113 (1991) 855.
[52] F. Kapteijn, L. Singoredjo, A. Andreini, J.A. Moulijn, Applied Catalysis B: Environmental 3 (1994) 173.
[53] P.R. Ettireddy, N. Ettireddy, S. Mamedov, P. Boolchand, P.G. Smirniotis, Applied Catalysis B: Environmental 76 (2007) 123.
[54] V. Houel, D. James, P. Millington, S. Pollington, S. Poulston, R. Rajaram, R. Torbati, Journal of Catalysis 230 (2005) 150.
[55] J. Li, R. Zhu, Y. Cheng, C.K. Lambert, R.T. Yang, Environmental Science and Technology 44 (2010) 1799.
[56] W.B. Li, J.X. Wang, H. Gong, Catalysis Today 148 (2009) 81.
[57] Z. Liu, P.J. Millington, J.E. Bailie, R.R. Rajaram, J.A. Anderson, Microporous and Mesoporous Materials 104 (2007) 159.
[58] S.T. Choo, S.D. Yim, I.-S. Nam, S.-W. Ham, J.-B. Lee, Applied Catalysis B: Environmental 44 (2003) 237.
[59] Z. Zhu, H. Niu, Z. Liu, S. Liu, Journal of Catalysis 195 (2000) 268.
[60] L. Mao, A. T-Raissi, C. Huang, N.Z. Muradov, International Journal of Hydrogen Energy 36 (2011) 5822.
[61] G. Xie, Z. Liu, Z. Zhu, Q. Liu, J. Ge, Z. Huang, Journal of Catalysis 224 (2004) 36.
[62] Z. Wu, R. Jin, H. Wang, Y. Liu, Catalysis Communications 10 (2009) 935.